The scale **Journal Website:** https://thescalejournal.com.ng/
An Interdisciplinary Journal of **https://doi.org/10.5281/zenodo.20280490**
The ACADEMIC STAFF UNION OF POLYTECHNICS - ZONE D
ISSN: 2992-3727 Published 30th May, 2026

VISIBLE-LIGHT-DRIVEN PHOTOCATALYTIC DEGRADATION OF PHENOL USING ZnO, α-FE_2O_3, AND $ZnFE_2O_4$-BASED COMPOSITE PHOTOCATALYSTS

Fatuase Johnson Tunde [1]; Udoye Benjamin Onyebuchi [1]
[1]Department of Chemical Engineering, Federal Polytechnic Oko, Anambra, Nigeria
Email: johnson.fatuase@federalpolyoko.edu.ng

Abstract
Phenol and its derivatives are persistent, toxic organic pollutants commonly found in industrial wastewater. This study investigates the synthesis, characterization, and visible-light photocatalytic activity of ZnO, α-Fe_2O_3, and $ZnFe_2O_4$-based composites (75Zn:25Fe, 50Zn:50Fe, and 25Zn:75Fe) for the degradation of phenol in aqueous solution. The photocatalysts were prepared via a simple co-precipitation method followed by calcination at 1000 °C and characterized by X-ray fluorescence (XRF), X-ray diffraction (XRD), and UV-V is spectroscopy. Photocatalytic experiments were conducted under natural sunlight and a 500 W halogen lamp (visible light) using 100 mg L^{-1} phenol solutions. Among the catalysts, pure α-Fe_2O_3 exhibited the highest photocatalytic efficiency, achieving 86% phenol degradation with a rate constant of 0.3108 min^{-1}. The activity order was α-Fe_2O_3 > 25Zn:75Fe > 50Zn:50Fe > 75Zn:25Fe > ZnO. Optimal conditions included acidic *p*H, 1.5 g L^{-1} catalyst loading, and low initial phenol concentration. Adsorption played a significant role and degradation followed the Langmuir–Hinshelwood kinetic model. These results demonstrated that low-cost, visible-light-active α-Fe_2O_3-based materials are promising for the treatment of phenolic wastewater using solar or artificial visible light.

Keywords: Photocatalysis; Phenol degradation; ZnO; α-Fe_2O_3; $ZnFe_2O_4$ composites; Visible light; Advanced oxidation process

1. Introduction

Photocatalysis has emerged as a sustainable advanced oxidation process (AOP) for the mineralization of refractory organic pollutants such as phenol, which is highly toxic, bio-recalcitrant, and widely present in industrial effluents (Galeas, *et al*, 2025). Conventional treatment methods are often ineffective or costly for complete degradation to safe levels (0.1–1 mg L^{-1}). Semiconductor photocatalysts generate electron-hole pairs under light irradiation, producing highly reactive hydroxyl radicals (·OH) that oxidize organic compounds to CO_2, H_2O, and inorganic acids (Sudhaik, *et al,* 2020). Titanium dioxide (TiO_2) is the most studied photocatalyst due to its stability and low cost; however, its wide bandgap (3.0–3.2 eV) limits activity to UV light (<5% of solar spectrum) (Cai, *et al,* 2016). To harness abundant visible sunlight, narrower-bandgap materials like ZnO (3.2 eV), α-Fe_2O_3 (2.2 eV), and their composites (e.g., $ZnFe_2O_4$) have been explored (Arimi,*et al,* 2018; Bayahia, 2022.; Behera*et al,* 2018). Composites can enhance charge separation, extend visible-light response, and improve stability (Li, *et al,* 2025; Wang, *et al,*2023; Zouheir, *et al,* 2020). Recent studies have highlighted the superior performance of spinel ferrites and ZnO/Fe2O3 heterostuctures under visible and solar irradiation for organic pollutant removal (Wu, and Song, 2023; Aina, *et al,* 2025 & Makota, *et al,* 2025).

This work focuses on the synthesis and evaluation of ZnO, α-Fe_2O_3, and ZnO–$ZnFe_2O_4$–Fe_2O_3 composites for visible-light-driven phenol degradation. The objectives were to synthesize the materials,

characterize them, test their photocatalytic performance under solar and halogen-lamp irradiation, and optimize key parameters (catalyst loading, initial phenol concentration, and pH).

2. Materials and Methods

2.1 Synthesis of Photocatalysts

ZnO, α-Fe_2O_3, and composite photocatalysts were synthesized by co-precipitation. Zinc nitrate hexahydrate (Zn $(NO_3)_2 \cdot 6H_2O$) and iron (III) nitrate nonahydrate ($Fe(NO_3)_3 \cdot 9H_2O$) were dissolved in deionized water. Ammonium hydroxide (NH_4OH) was added dropwise under vigorous stirring at 50 °C to maintain pH 8, forming metal hydroxides. The precipitates were aged for 24 h, washed, vacuum-filtered, dried at 110 °C overnight, and calcined at 1000 °C for 4 h to obtain the oxide forms. Composites were prepared at molar ratios of 95:5, 75:25, 50:50, and 25:75 (Zn:Fe). The relevant reactions are:

$$Fe(NO_3)_3 \cdot 9H_2O + 3NH_4OH \rightarrow Fe(OH)_3 + 3NH_4NO_3 + 9H_2O \quad (1)$$

$$Zn(NO_3)_2 \cdot 6H_2O + 2NH_4OH \rightarrow Zn(OH)_2 + 2NH_4NO_3 + 6H_2O \quad (2)$$

Calcination:

$$2Fe(OH)_3 \rightarrow Fe_2O_3 + 3H_2O \quad (3)$$

$$Zn(OH)_2 \rightarrow ZnO + H_2O \quad (4)$$

$$\text{Mixed hydroxides} \rightarrow ZnO + ZnFe_2O_4 + Fe_2O_3 \quad (5)$$

2.2 Characterization

Chemical composition was determined by X-ray fluorescence (XRF, Minipal 4). Crystal structure was analyzed by X-ray diffraction (XRD, Empyrean). Specific surface area was measured using a modified BET method with saturated salt solutions ($CaSO_4$, K_2SO_4, CH_3COONa, $MgCl_2$) to establish relative humidity. UV-V is spectrophotometry (Jenway 6405) was used to monitor phenol concentration at its λ_max.

2.3 Photocatalytic Experiments

Stock phenol solution (100 mg L^{-1}) was prepared in deionized water. Experiments used 200 mL solution in a reactor with 0.1–3.0 g L^{-1} catalyst loading. The suspension was stirred in the dark for 2 h to reach adsorption–desorption equilibrium, then irradiated under natural sunlight (monitored by lux meter) or a 500 W halogen lamp. Aliquots (5 mL) were withdrawn at intervals, filtered, and analyzed by UV-V is spectrophotometry. Parameters optimized included catalyst loading, initial phenol concentration, and *p*H. All experiments were performed in duplicate. Dark adsorption tests were conducted separately.

3. Results and Discussion

3.1 Chemical Composition and Crystal Structure

XRF analysis (Table 1) confirmed high purity: ZnO contained ~99.2% ZnO, α-Fe_2O_3 ~97.9% Fe_2O_3, with composites showing expected Zn/Fe ratios and minor impurities (SiO_2, CaO, etc.).

Table 1 XRF results showing Chemical Composition of the synthesized Photocatalysts (% wt.)

ZnO	Compound	CaO	Cr_2O_3	Fe_2O_3	NiO	ZnO	Pr_2O_3	Eu_2O_3	Er_2O_3	Yb_2O_3
	Conc	0.10	0.041	0.015	0.01	99.19	0.23	0.062	0.086	0.25
	Unit	%	%	%	%	%	%	%	%	%
75Zn:25Fe	Compound	SiO_2	P_2O_5	SO_3	CaO	Cr_2O_3	Fe_2O_3	NiO	ZnO	La_2O_3
	Conc	0.69	0.25	0.17	0.056	46.29	0.02	52.1	0.16	0.09
	Unit	%	%	%	%	%	%	%	%	%
50Zn:50Fe	Compound	SiO_2	P_2O_5	SO_3	CaO	Cr_2O_3	Fe_2O_3	ZnO	Ag_2O	La_2O_3
	Conc	0.36	0.24	0.15	0.095	0.052	78.31	18.6	1.87	0.30
	Unit	%	%	%	%	%	%	%	%	%
25Zn:75Fe	Compound	P_2O_5	CaO	Sc_2O_3	Cr_2O_3	Fe_2O_3	ZnO	Ag_2O	La_2O_3	-
	Conc	0.18	0.094	0.02	0.049	90.06	7.62	1.75	0.24	-
	Unit	%	%	%	%	%	%	%	%	%
Fe_2O_3	Compound	CaO	Sc_2O_3	Cr_2O_3	Fe_2O_3	ZnO	Ag_2O	La_2O_3	Re_2O_7	-
	Conc	0.093	0.020	0.058	97.85	0.22	1.45	0.21	0.1	-
	Unit	%	%	%	%	%	%	%	%	%

XRD patterns (Figs. 1–5) revealed:
- Pure ZnO: wurtzite (zincite) phase.
- Pure α-Fe_2O_3: hematite phase.
- Composites: mixed phases of ZnO (zincite), $ZnFe_2O_4$ (franklinite), and α-Fe_2O_3 (hematite), with increasing hematite/franklinite peaks as Fe content rose.

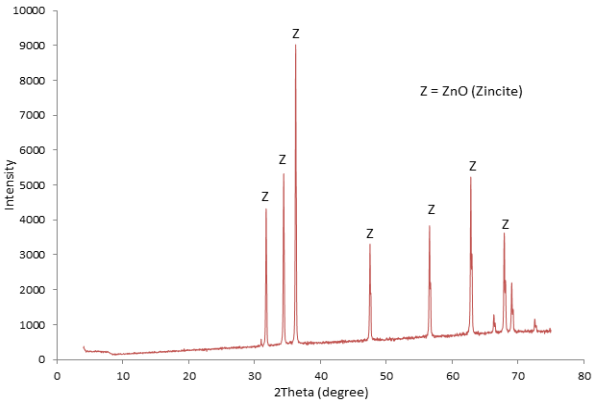


Fig 1. XRD pattern of ZnO photocatalyst calcined at 1000°C

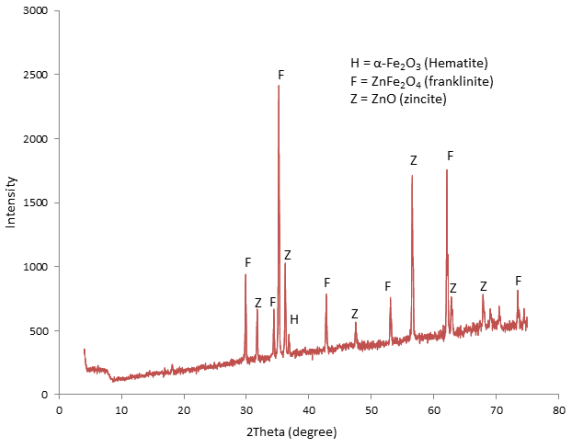


Fig 2. XRD pattern of 75Zn:25Fe (ZnO-$ZnFe_2O_4$ composite) catalyst calcined at 1000°C

The scale Journal Website: https://thescalejournal.com.ng/
An Interdisciplinary Journal of https://doi.org/10.5281/zenodo.20280490
The ACADEMIC STAFF UNION OF POLYTECHNICS - ZONE D
ISSN: 2992-3727 Published 30th May, 2026

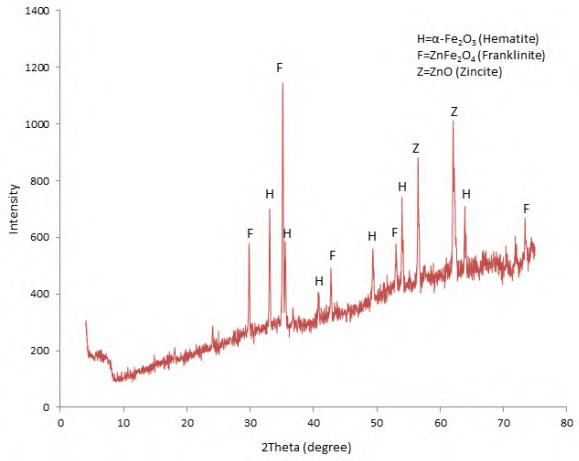


Fig 3. XRD pattern of 50Zn:50Fe (ZnO-$ZnFe_2O_4$-Fe_2O_3 composite) catalyst calcined at 1000°C

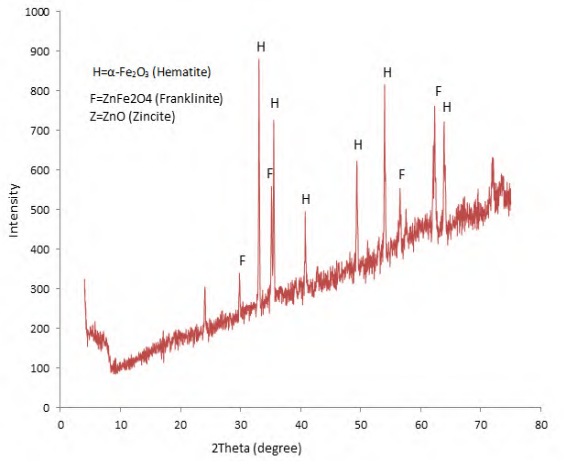


Fig 4. XRD pattern of 25Zn:75Fe ($ZnFe_2O_4$-Fe_2O_3) composite photocatalyst calcined at 1000°C

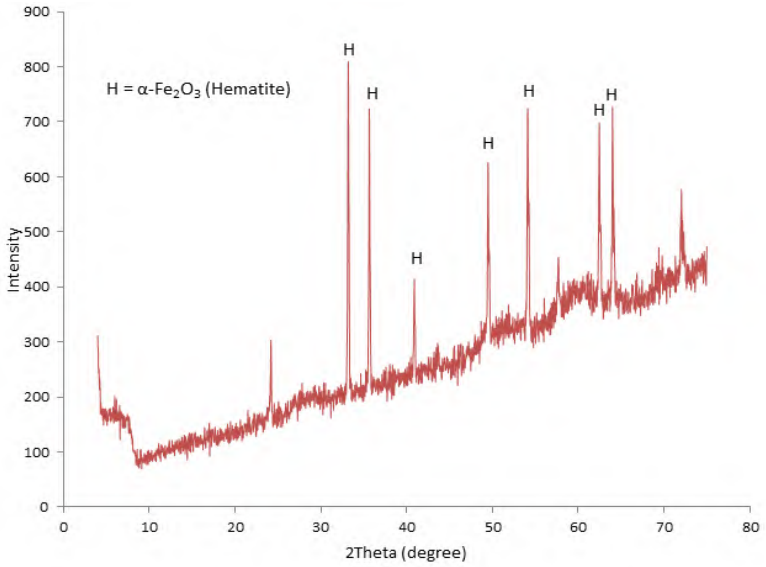


Fig 5. XRD pattern of Fe_2O_3 photocatalyst calcined at 1000°C

These phases are consistent with visible-light-active semiconductors suitable for photocatalysis. (Bayahia, 2022; Behera, *et al*, 2018; Li, *et al,* 2025; Zouheir *et al*, 2020)

3.2 Photocatalytic Degradation of Phenol

Under visible-light irradiation, phenol degradation followed the order: α-Fe_2O_3 (86%) > 25Zn:75Fe (70%) > 50Zn:50Fe (66%) > 75Zn:25Fe (61%) > ZnO (52%). α-Fe_2O_3 showed the fastest kinetics (k = 0.3108 min^{-1}). The superior performance of α-Fe_2O_3 is attributed to its narrower band-gap (~2.2 eV), enabling efficient visible-light absorption, and favorable charge separation (Arimi, *et al,* 2018; Cai, *et al,* 2016). Composites benefited from hetero-junction formation, reducing electron-hole recombination,

but pure α-Fe_2O_3 outperformed them, consistent with recent reports on $ZnFe_2O_4$ - based systems (Bayahia, 2022; Behera , *et al,* 2018; Makota, *et al,* 2025).

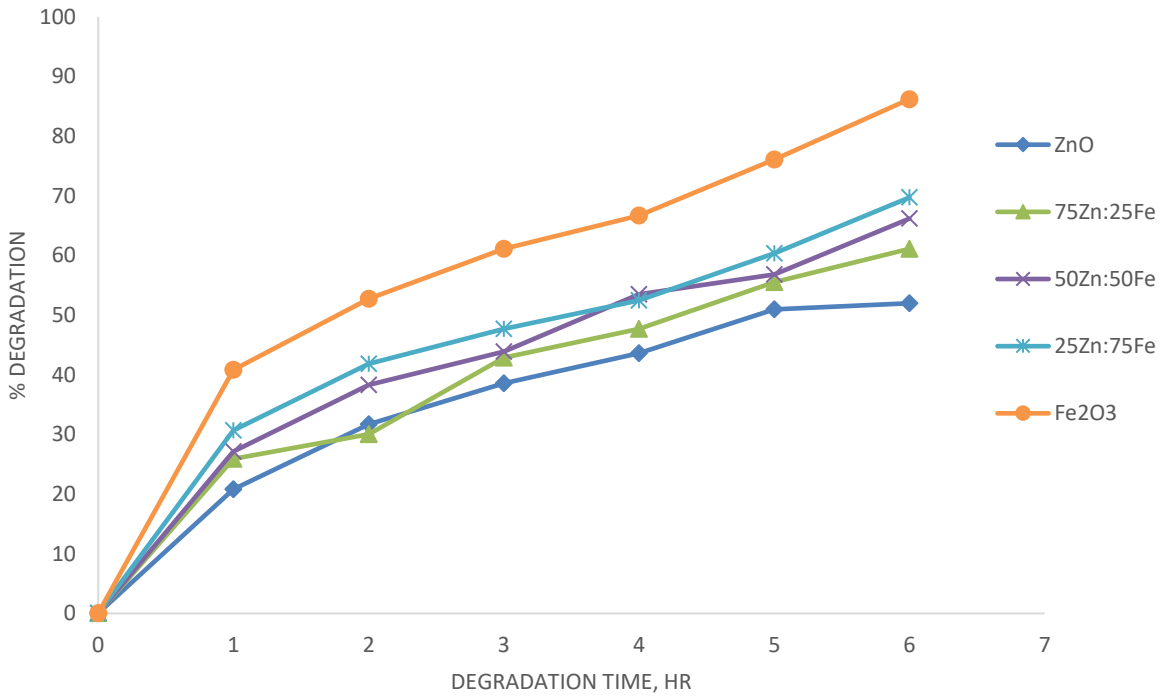


Fig. 6. Percentage Degradation of phenol solution with the photocatalyst

Adsorption in the dark contributed significantly to overall removal. Degradation kinetics obeyed the Langmuir–Hinshelwood model, indicating surface-reaction control (Jin *et al,* 2023).

3.3 Effect of Operational Parameters

- **Catalyst loading:** Degradation rate increased with loading up to an optimum (1.5 g L^{-1} for α-Fe_2O_3), beyond which light scattering and agglomeration reduced efficiency (Wu, *et al*, 2023; Aina, *et al*, 2025).

The scale Journal Website: https://thescalejournal.com.ng/
An Interdisciplinary Journal of https://doi.org/10.5281/zenodo.20280490
The ACADEMIC STAFF UNION OF POLYTECHNICS - ZONE D
ISSN: 2992-3727 Published 30th May, 2026

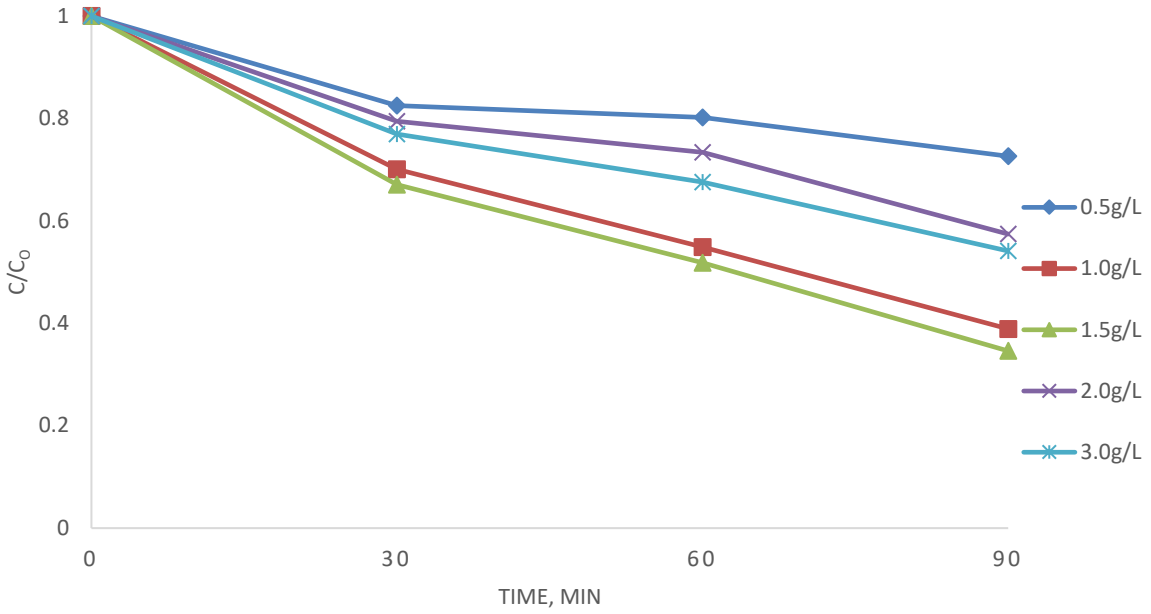


Fig 7. Photocatalytic degradation of phenol with different Fe_2O_3 loadings at different time intervals of irradiation

- **Initial phenol concentration:** Lower concentrations (e.g., 0.5 g L^{-1}) favored higher % removal due to sufficient ·OH availability; higher concentrations led to competition for active sites and intermediate accumulation (Galeas, *et al*, 2025).

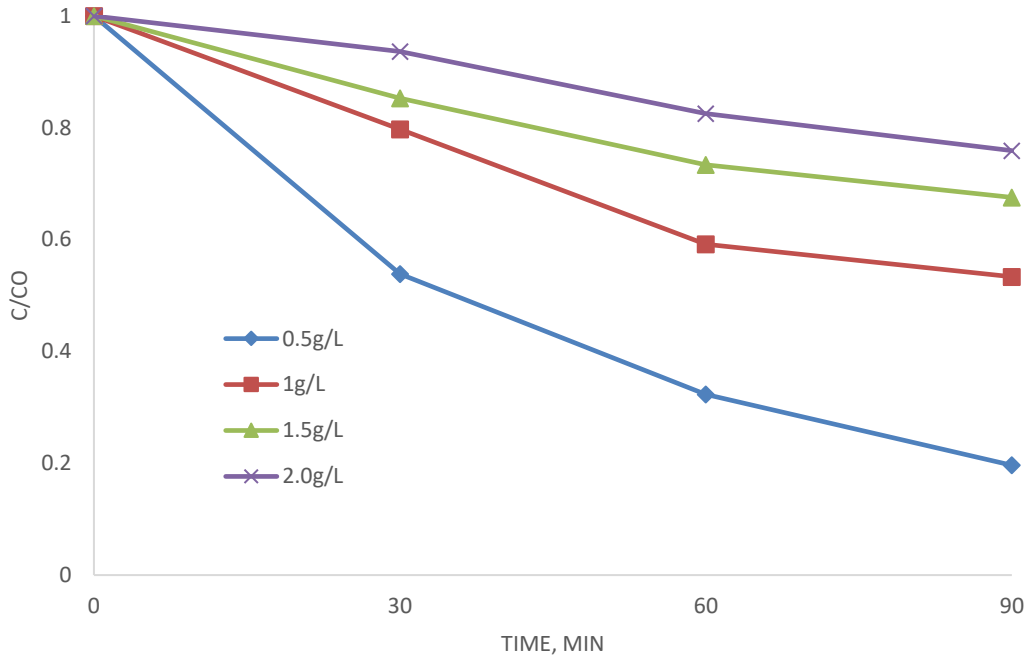


Fig 8. Photocatalytic degradation of phenol with different phenol concentration

- ***p*H:** Maximum degradation occurred in acidic medium, where the catalyst surface charge and phenol presence enhanced adsorption and radical formation (Wu, and Song, 2023).

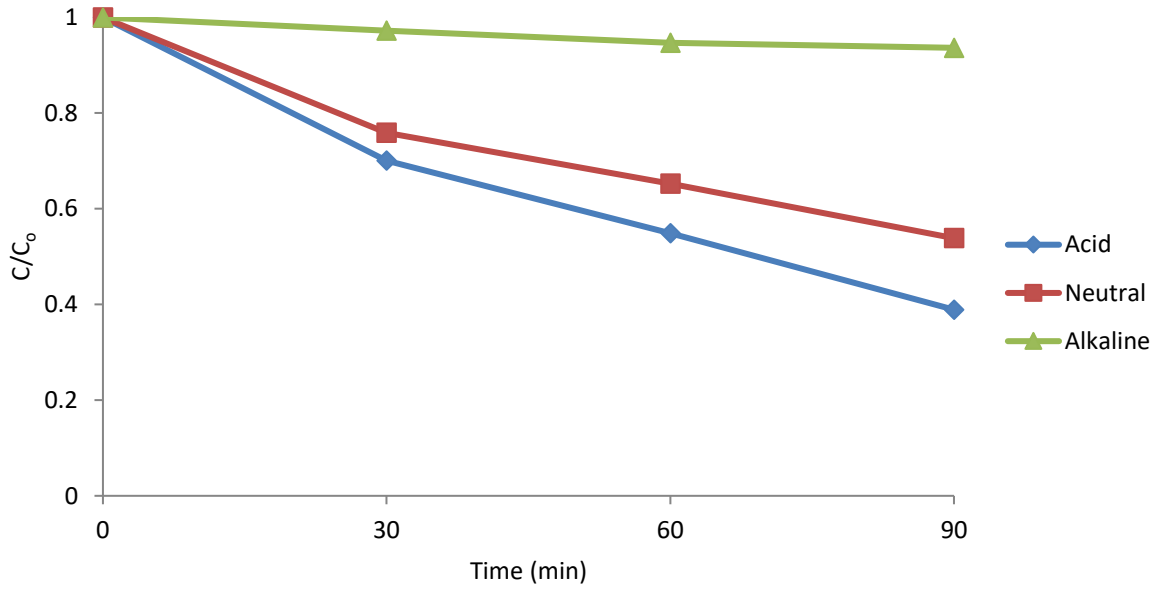


Fig 9. Effect of pH on the photocatalytic degradation of phenol using α-Fe_2O_3 (C_o: initial phenol concentration, C: phenol concentration at time t)

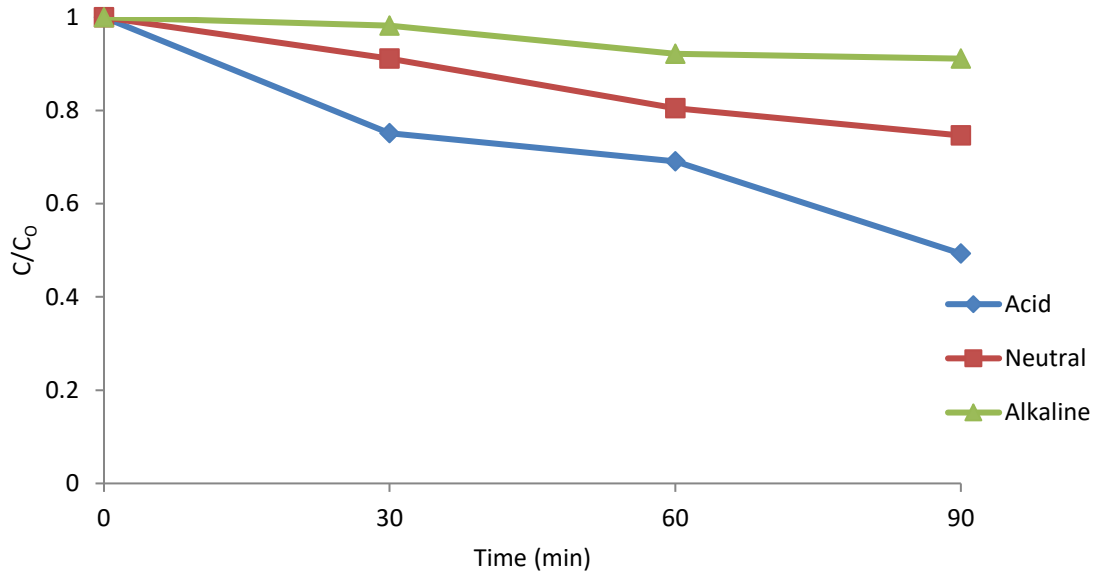


Fig 10. Effect of pH on the photocatalytic degradation of phenol using 50Zn:50Fe (C_o: initial phenol concentration, C: phenol concentration at time t)

UV-Vis analysis confirmed progressive decrease in phenol absorbance, supporting mineralization. These findings align with recent advances in magnetically separable ZnO/Fe_2O_3 heterostructures for efficient visible-light phenol degradation (Makota, *et al,* 2025; Sabar, *et al*, 2025).

4. Conclusion

ZnO, α-Fe_2O_3, and $ZnFe_2O_4$-based composites were successfully synthesized by co-precipitation and calcination. α-Fe_2O_3 proved the most effective visible-light photocatalyst for phenol degradation (86% removal), outperforming ZnO and the composites (Bayahia, 2022; Behera, *et al*, 2018; Li, *et al*, 2025). The process is efficient under solar or halogen-lamp irradiation, follows Langmuir–Hinshelwood kinetics, and is enhanced by adsorption (Galeas, *et al*, 2025; Jin, *et al*, 2023). This low-cost, environmentally friendly approach offers a viable alternative for treating phenolic industrial wastewater using renewable solar energy (Aina, *et al,* 2025; Jin, *et al,* 2023)

5. References

1. Ahmed, S., et al. (2011). Advances in heterogeneous photocatalysis for water treatment. *Journal of Environmental Management*, 92(3), 400–420.
2. Arimi, A., Megatif, L., Granone, L.I, Dillert, R.,and Bahnemann, D. (2018). Visible-light photocatalytic activity of zinc ferrites. *Journal of Photochemistry and Photobiology A: Chemistry*, 366, 118–126.
3. Bayahia, H. (2022). High activity of $ZnFe_2O_4$ nanoparticles for photodegradation of crystal violet dye solution in the presence of sunlight. *Journal of Taibah University for Science*, 16(1), 988-1004.
4. Behera, A., Kandi, D, Majhi, SM, Martha, S., and Parida, K. (2018). Facile synthesis of $ZnFe_2O_4$ photocatalysts for decolourization of organic dyes under solar irradiation. *Beilstein Journal of Nanotechnology*, 9(15), 436–446.
5. Cai, C., Zhang, Z., Liu, J., Shan, N., Zhang, H. and Dionysiou, D. (2016). Visible light-assisted heterogeneous Fenton with $ZnFe_2O_4$ for the degradation of organic pollutants. *Applied Catalysis B: Environmental*, 182, 456–468.
6. Chaves, N.O., Monteiro, M.D., Lira, T.M., Santos, D.B., *et al.* (2025). Sunlight-driven photocatalysis in hydrothermally coupled ZnO/Fe_3O_4 heterostructures from bioengineered nanoparticles. *Nanomaterials*, 15(24), 1864.
7. Feng, X., Guo, H., Patel, K., and Zhou, H. (2014). High performance, recoverable Fe_3O_4/ZnO nanoparticles for phenol degradation. *Chemical Engineering Journal*, 244, 327–334.
8. Gogoi, D., Makkar, P. and Ghosh, N.N.. (2021). Solar light-irradiated photocatalytic degradation of model pollutants using g-C_3N_4/$CoFe_2O_4$ composites. *ACS Omega*, 6(12), 8452–8463.
9. Li, L., Jianhua, W. and Fang, H. (2025). Fabrication of $ZnFe_2O_4$@g-C_3N_4 for enhanced photo-Fenton effect and visible light-driven organic dye degradation. *Scientific Reports*, 15, 21707.
10. Mady, A.H., Baynosa, M.L., Tuma, D. and Shim, J. (2023). Heterogeneous activation of peroxymonosulfate by a novel magnetic 3D γ-MnO_2@$ZnFe_2O_4$/rGO nanohybrid for phenol degradation. *Journal of Environmental Chemical Engineering*, 11(3), 109850.
11. Safizade, B., Masoudpanah, S.M., Hasheminiasari, M and Ghasemi, A. (2018). Photocatalytic activity of $BiFeO_3$/$ZnFe_2O_4$ nanocomposites under visible light. *Scientific Reports*, 12, 9078354.

12. Wang, L., Liu, S., Lu, J., Yuan, Z., Gao, D. and Li, Y. (2023). Construction of $ZnFe_2O_4$/g-C_3N_4 nanocomposite catalyst for enhanced photo-Fenton reaction. *Materials Today Sustainability*, 22, 100201.
13. Wu, Q., and Song, Y. (2023). Recent advances in spinel ferrite-based magnetic photocatalysts for efficient degradation of organic pollutants. *Chemical Engineering Journal*, 456, 141234.
14. Zouheir, M., Tanji, K., Navio, J.A. and Hidalgo ,M.C (2020). Preparation of $ZnFe_2O_4$/ZnO composite: Effect of operational parameters for photocatalytic degradation of dyes under UV and visible illumination. *Journal of Photochemistry and Photobiology A: Chemistry*, 390, 112305.
15. Aina, A.R.N., Patel, H., Aich, S. and Roy, B. (2025). Recent advances in ZnO based photocatalysts for industrial wastewater treatment. *Discover Applied Sciences*, 7, 7530.
16. Ahmed, Z.M., Allam, A.A. El-SAyed, M., El-Gaied, I.M., Salama, Y., Rudanyi, H.A. Zoubi, W. and Abukhadra, M.R. (2026). Visible-light photocatalytic mineralization of 4-chlorophenol over ZnO-loaded sulfonated carbonaceous bentonite. *Scientific Reports*, 16, 35956.
17. Bouziani, M., Bouziani, A., Hsini, A and Bianchi, C.. (2026). Development of visible-light-active Fe_2O_3-hBN photocatalysts for organic pollutant degradation. *Journal of Hazardous Materials Advances*, 14, 100063X.
18. Galeas, S., Guerrero, V.H., ponton, P.I. and Goetz, V. (2025). Visible light-driven phenol degradation via advanced oxidation processes: Kinetic study. *Molecules*, 30(9), 2059.
19. Jin, Z., Cui, J., Xu, C., Liu, H., Hu, R. and Liu, F. (2023). Visible light photocatalysis: Efficient Z-scheme $LaFeO_3$/g-C_3N_4/ZnO photocatalyst for phenol degradation. *Environmental Science and Pollution Research,* 30(43):1-16.
20. Makota, O., Lisnichuk, M., Briancin, J. Bednarcik, J., Bondarchuk, O. and Melnyk, I. (2025). Magnetically enhanced Fe_3O_4@ZnO composites for efficient UV and visible light photodegradation. *Chemosphere*, 377, 144365.
21. Sabar, S., Jamil, A., Zhao, Y., Yusof, N.M. (2025). Construction of Fe_3O_4/ZnO heterostructure photocatalysts for enhanced photocatalytic degradation. *New Journal of Chemistry*, 49, 8267–8278.
22. Sudhaik, A., Sharma, K., Sudahiak, A., and Raizada, P. (2020). Magnetically separable ZnO/$ZnFe_2O_4$ photocatalysts supported onto nitrogen doped graphene for toxic dye degradation (phenol extensions). *Journal of Environmental Chemical Engineering*, 8(5), 104298.
23. Vikas, V. and Rana, P.S. (2023). Solar driven photocatalysis using $CoFe_2O_4$-CNT for organic pollutant removal. *Journal of Water and Environmental Nanotechnology*, 8(3), 705283.
24. Fujishima, A. and Zhang X. (2008). Titanium dioxide photocatalysis: Present situation and future approaches. *Comptes Rendus Chimie*, 11(1-2), 215–229.